

# $^{29}\text{Si}$ and $^{27}\text{Al}$ MAS NMR spectra of mullites from different kaolinites

Hongping He<sup>a,\*</sup>, Jiugao Guo<sup>a</sup>, Jianxi Zhu<sup>a</sup>, Peng Yuan<sup>a</sup>, Cheng Hu<sup>b</sup>

<sup>a</sup> Guangzhou Institute of Geochemistry, Chinese Academy of Sciences, Wushan, Guangzhou 510640, China

<sup>b</sup> National Laboratory of Solid State Microstructural Physics, Nanjing University, Nanjing 210093, China

Received 16 June 2003; received in revised form 25 July 2003; accepted 25 July 2003

## Abstract

Mullites synthesized from four kaolinites with different random defect densities have been studied by  $^{27}\text{Al}$  and  $^{29}\text{Si}$  magic angle spinning nuclear magnetic resonance spectroscopy (MAS NMR) and X-ray diffraction (XRD). All these mullites show the same XRD pattern. However,  $^{29}\text{Si}$  and  $^{27}\text{Al}$  MAS NMR spectra reveal that the mullites derived from kaolinites with high defect densities, have a sillimanite-type Al/Si ordering scheme and are low in silica, whereas those mullites derived from kaolinites with low defect densities, consist of both sillimanite- and mullite-type Al/Si ordering schemes and are rich in silica.

© 2003 Elsevier B.V. All rights reserved.

**Keywords:** MAS NMR spectrum; Mullite; Kaolinite; Defect density

## 1. Introduction

Mullite is an important and widely studied ceramic material. It is used in a diverse number of applications, including structural and refractory ceramics, microelectronic packaging, high-temperature protective coatings, microwave dielectrics, and infrared-transmitting materials [1,2]. In the kaolinite–mullite reaction sequence, mullite begins to form around 980 °C and the amount of mullite increases with increasing temperature [3–11]. However, from previously reported data, there are obvious variations among the different  $^{29}\text{Si}$  and  $^{27}\text{Al}$  magic angle spinning nuclear magnetic resonance spectroscopy (MAS NMR) spectra. Sanz et al. [5] reported three  $^{27}\text{Al}$  resonances at 0 ppm ( $\text{Al}^{\text{VI}}$ ), 42 ppm ( $\text{Al}^{\text{IV}}$ ), and 60 ppm ( $\text{Al}^{\text{IV}}$ ). Other researchers [6,10,11] revealed only two  $^{27}\text{Al}$  signals corresponding to  $\text{Al}^{\text{IV}}$  and  $\text{Al}^{\text{VI}}$ . Rocha et al. [7] considered that the signal at ca. 44 ppm would be observed by changing the spinning frequency of the MAS rotor thereby removing the spinning sidebands. Massiot et al. [10] proposed that the lack of resolution of the two tetrahedral Al was linked to the structural disorder ( $\text{Si}^{\text{IV}}/\text{Al}^{\text{IV}}$ ) and the associated oxygen vacancies. Simultaneously, these researchers suggested that the initial mullite was silica poor,

and that  $^{29}\text{Si}$  signal at  $-87$  ppm is related to mullite. All previous  $^{29}\text{Si}$  MAS NMR studies of kaolinite–mullite reaction series did not report the  $^{29}\text{Si}$  signals of mullite at  $-90$  and  $-94$  ppm, which were identified in the sinter-mullite and the fused-mullite [12].

It is obvious that variations of  $^{27}\text{Al}$  and  $^{29}\text{Si}$  signals could be due to sample variation. Most studies used only one or two kaolinites. In this study, four kaolinite samples with different random defect densities were used as starting materials. Mullites were synthesized at similar experimental conditions and their microstructures were principally studied by using  $^{29}\text{Si}$  and  $^{27}\text{Al}$  MAS NMR spectroscopy. Our research objective is to reveal the effect of the characteristics of parent kaolinites on the microstructures of the derived mullites.

## 2. Samples and methods

The chemical compositions of the four parent kaolinites (K1, K2, K3, and K4) are shown in Table 1. Evaluated from XRD and chemical analysis results, quartz is the main impurity (<3%) in K1, K3, and K4. In addition, K1 contains minor anatase and K4 shows minor illite. K2 is a kaolinite taken from coal bed and contains 3% organic materials. The  $R_2$  index of Lietard, reflecting the random defect density of kaolinite, was calculated from the intensities of (1 3 1) and (1  $\bar{3}$  1) peaks, in the range 37–40°  $2\theta$  Cu K $\alpha$  as

\* Corresponding author. Tel.: +86-20-85290257; fax: +86-20-85290130.

E-mail address: [hehp@gig.ac.cn](mailto:hehp@gig.ac.cn) (H. He).

Table 1  
Chemical compositions of the four parent kaolinite samples

Sample	SiO <sub>2</sub>	TiO <sub>2</sub>	Al <sub>2</sub> O <sub>3</sub>	Fe <sub>2</sub> O <sub>3</sub>	MnO	MgO	CaO	Na <sub>2</sub> O	K <sub>2</sub> O	H <sub>2</sub> O	Total
K1	47.80	0.99	36.55	0.30	–	0.17	0.11	0.11	0.02	13.59	99.64
K2	45.63	0.45	38.21	0.12	–	0.07	0.09	0.09	0.03	14.28	98.97
K3	47.51	0.29	38.22	0.01	–	0.06	0.13	0.30	0.12	13.87	100.51
K4	46.61	0.11	36.57	0.40	–	0.13	0.08	0.13	0.65	14.25	98.93
Average	46.51		39.53							13.95	99.99

shown in [13]. The  $R_2$  index of Lietard is only sensitive to the random defects and is an independent index (no relation with Hinckley index) that decreases with the increase of the monoclinic character of kaolinite. Well-resolved (1 3 1) and (1  $\bar{3}$  1) reflections indicate triclinic character and correspond to a high  $R_2$  value whereas the overlapping of the two peaks indicates monoclinic character and corresponds to a low  $R_2$  value. The  $R_2$  of natural kaolinites is in the range 0.3 (high defect) to 1.2 (low defect) [13]. The  $R_2$  indices for K1, K2, K3, and K4 are 0.77, 0.70, 0.62, and 0.62, respectively.

The samples were ground in a mortar so as to pass through a 200 mesh sieve before thermal treatments and various analysis. Thermal treatments of the parent kaolinites were carried out on LCT-2 differential thermobalance in the range 350–1200 °C. The samples were heated from room temperature to appointed high temperatures at a heating rate of 20 °C min<sup>-1</sup> and then kept at the appointed temperatures for 1 h. The thermal treatments above 1200 °C were performed in Pt muffle. Then the calcined samples were quenched in air and ground in a mortar so as to pass through a 200 mesh sieve. The products heated at 1300 °C for K1, K2, K3, and K4 were marked as M1, M2, M3, and M4, respectively, in which mullite and cristobalite are the main components.

XRD patterns of the samples were acquired on unoriented samples with a D/MAX-III A diffractometer using Cu K $\alpha$  radiation. <sup>29</sup>Si and <sup>27</sup>Al MAS NMR spectra of the samples were measured with a Bruker MSL-300 NMR spectrometer 59.6 and 78.2 MHz, respectively, using TMS as external reference with a 2  $\mu$ s pulse width and a 30 s recycle delay and using solution of AlCl<sub>3</sub> as external standard reference with a 0.6  $\mu$ s pulse width and a 0.2 s recycle delay, respectively. Rotors were spun in air at 4–5 KHz. The decompositions of <sup>27</sup>Al and <sup>29</sup>Si MAS NMR spectra were performed by PEAKFIT simulation program.

### 3. Results and discussion

XRD patterns show that a relatively large amount of mullite is present in K2, K3, and K4 at 1200 °C. The formation temperature of mullite in K2, K3, and K4 is 100 °C lower than that in K1, in which mullite was formed at 1300 °C. This indicates that mullite can form at lower temperature in parent kaolinite with high defect density than that with low defect density. With increasing temperature, the splitting of ( $h k 0$ ) and ( $k h 0$ ) of mullite occurs. It shows that the primary

mullite transforms into orthorhombic mullite (3/2-mullite) [9]. XRD patterns of mullite in M1, M2, M3, and M4 are identical and similar to previous reports [1,5,7].

<sup>29</sup>Si MAS NMR spectra show that the <sup>29</sup>Si signal of mullite at ca. –87 ppm increases gradually with increasing temperature while that of cristobalite at ca. –112 ppm decreases. This reflects increased mullite formation with silica consumption. Fig. 1 shows the experimental and simulated <sup>29</sup>Si and <sup>27</sup>Al MAS NMR spectra of M1, M2, M3, and M4.

<sup>29</sup>Si MAS NMR spectra shows that, in M3 and M4, the <sup>29</sup>Si signal of cristobalite is much stronger than that of mullite whereas the <sup>29</sup>Si signal of cristobalite is much weaker than that of mullite in M1 and M2. A signal at ca. –106 ppm corresponding to Q<sup>4</sup>Si (amorphous silica) presents in M3 and M4 but not in M1 and M2. Simulated spectra show that the ratios of Si atoms in mullite to those in cristobalite and amorphous silica in M1, M2, M3, and M4 are 66:34, 72:28, 39:61, and 44:56, respectively. This implies that the mullite in M1 and M2 is rich in silicon while that in M3 and M4 poor in silicon. <sup>29</sup>Si MAS NMR spectra of mullite in M3 and M4 display only one signal centered at ca. –87 ppm as indicated in previous studies [5–8,11,12], while mullite in M1 and M2 displays three <sup>29</sup>Si signals centered at ca. –87, –90, and –94 ppm, respectively. Sheriff and Grundy [14] have reported a correlation between <sup>29</sup>Si MAS NMR chemical shift data and the local geometry around Si in silicate structures. Applying that correlation, they calculated a chemical shift of –86.1 ppm for sillimanite, which is in good agreement with our experimental results. Therefore, the main signal at –87 ppm observed in all <sup>29</sup>Si spectra suggests a sillimanite-type Al/Si ordering scheme existing in mullite derived from these kaolinites. This also confirms the well-known structural similarity between mullite and sillimanite. The mullite structure can be derived from that of sillimanite by operation of the substitution O<sup>2-</sup> + 2Si<sup>4+</sup> → 2Al<sup>3+</sup>. This operation results in removing away some oxygens from the structure [12,15–17].

In commensurate systems the number of resonances in the NMR spectrum equals the number of physically non-equivalent nuclei per unit cell. In incommensurate systems where no translational lattice periodicity exists that number is essentially infinite. One thus expects a quasi-continuous distribution of NMR frequencies instead of discrete resonances. The nature of this distribution depends critically on the space variation of the phase of the incommensurate modulation, i.e. the NMR spectrum of

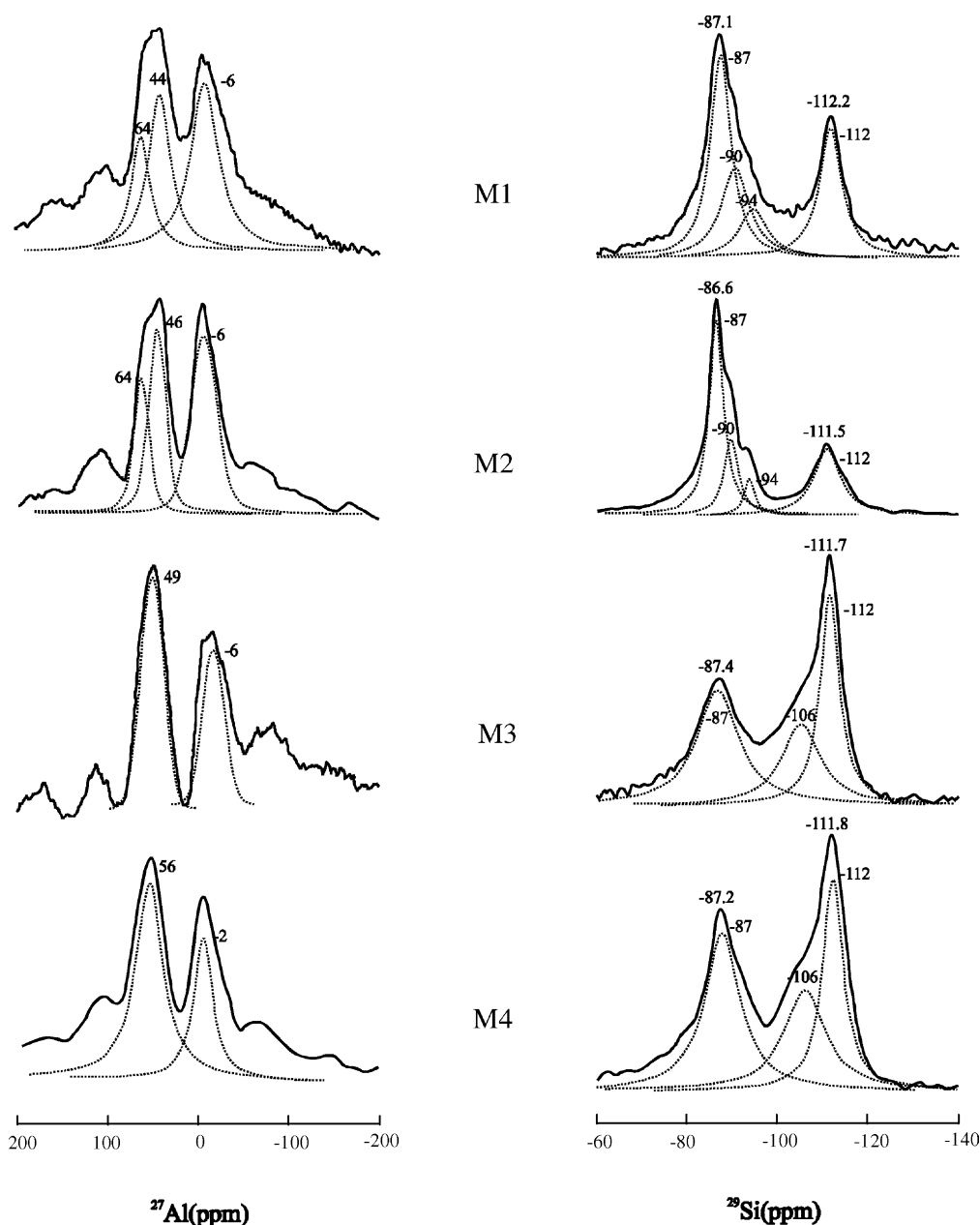


Fig. 1. The experimental and simulated  $^{27}\text{Al}$  and  $^{29}\text{Si}$  MAS NMR spectra of M1, M2, M3, and M4. Solid lines: experimental spectra; dotted lines: simulated spectra.

incommensurate systems may consist of so-called commensurate and incommensurate resonances [12,18]. Taking this into account the  $^{29}\text{Si}$  MAS NMR spectra of mullite may be interpreted as follows: the  $^{29}\text{Si}$  resonance at  $-87$  ppm might be attributed to locally commensurate domains in mullite whereas the resonance at  $-90$  and  $-94$  ppm were possibly incommensurate resonances reflecting the incommensurate properties of mullite. Merwin et al. [12] proposed that the resonance at  $-94$  ppm might result from Si atoms having a mullite type Al/Si ordering, i.e. having Si in the Si(3Al) region, in which one oxygen atom is shared by three surrounding Al tetrahedra. It suggests that mullite derived

from K3 and K4 contained sillimanite-type Al/Si ordering while that from K1 and K2 contained both sillimanite- and mullite-type Al/Si ordering. This seems to contradict with our proposal that mullite derived from K1 and K2 is richer in silicon than that from K3 and K4 because sillimanite generally is richer in silicon than mullite. We believe that this might be explained by the distribution of Al and Si in the two tetrahedral sites of mullite, i.e. there might be more Si atoms occupying tetrahedral sites in mullite from K1 and K2. This explanation is supported by the  $^{27}\text{Al}$  MAS NMR spectra, as shown less amount of aluminum atoms in tetrahedral sites of mullite in M1 and M2 than that in M3 and

M4. Simultaneously, the comparison of  $^{29}\text{Si}$  MAS NMR spectra shows that FWHM (full-width-at-half-maximum) of mullite signal at  $-87$  ppm in M3 and M4 is larger than that in M1 and M2. This result indicates that the distributions of Al and Si atoms in mullite of M3 and M4 are more “disordered” than those of M1 and M2.

$^{27}\text{Al}$  MAS NMR spectra of M1 and M2 display three mullite signals at ca.  $-6$  ppm,  $45$  ppm and  $64$  ppm, respectively. The first mullite signal corresponds to 6-coordinated Al and the other two to 4-coordinated Al. The  $^{27}\text{Al}$  signal at ca.  $45$  ppm should be assigned to aluminum tetrahedra in mullite, in which one oxygen atom is shared by three surrounding Al tetrahedra as proposed by Merwin et al. [12]. Simulated spectra exhibit that the ratios of  $\text{Al}^{\text{VI}}$  ( $-6$  ppm) and  $\text{Al}^{\text{IV}}$  ( $45$  and  $64$  ppm) in M1 and M2 are 46:32:22 and 46:34:20, respectively. However, spectrum of mullite displays only two  $^{27}\text{Al}$  signals centered at ca.  $-6$  ppm and  $49$  ppm in M3 and at ca.  $-2$  ppm and  $56$  ppm in M4. The ratios of  $\text{Al}^{\text{VI}}$  and  $\text{Al}^{\text{IV}}$  in the mullite of M3 and M4, evaluated by the simulated spectra, are 39:61 and 35:65, respectively. By comparison of the ratio of  $\text{Al}^{\text{VI}}$  and  $\text{Al}^{\text{IV}}$  in mullite, we find that there is less amount of aluminum atoms occupying tetrahedral sites of mullite in M1 and M2 than that in M3 and M4. It proves that the mullites in M1 and M2 are relatively richer in silicon than those in M3 and M4. We conclude that the random defect densities of parent kaolinites play a prominent effect on microstructures and components of mullites.

#### 4. Conclusion

Our results suggest that the random defect densities of parent kaolinites play a prominent effect on microstructures and components of mullites. Mullite derived from kaolinite with high random defect density has a sillimanite-type Al/Si ordering scheme and is rich in aluminum, whereas that with

low random defect density consists of both sillimanite- and mullite-type Al/Si ordering schemes and is rich in silica.

#### Acknowledgements

We are most grateful to National Natural Science Foundation of China (49972018) and Natural Science Foundation of Guangdong Province (990522) for financial support. Prof. R.L. Frost, Dr. Chen Min and Dr. Xu Youshen are thanked for useful discussions and review.

#### References

- [1] P. Kansal, R.M. Laine, *J. Am. Ceram. Soc.* 80 (1997) 2597.
- [2] R. Soundararajan, G. Kuhn, R. Atisivan, S. Bose, A. Bandyopadhyay, *J. Am. Ceram. Soc.* 84 (2001) 509.
- [3] G.W. Brindley, M. Nakahira, *J. Am. Ceram. Soc.* 42 (1959) 319.
- [4] H.J. Percival, J.F. Duncan, P.K. Foster, *J. Am. Ceram. Soc.* 59 (1974) 57.
- [5] J. Sanz, A. Madani, J.M. Serratos, *J. Am. Ceram. Soc.* 71 (1988) c418.
- [6] J. Rocha, J. Klinowski, *Phys. Chem. Miner.* 17 (1990) 179.
- [7] J. Rocha, J. Klinowski, J.M. Adams, *J. Mater. Sci.* 26 (1991) 3009.
- [8] H. Hongping, H. Cheng, G. Jiugao, W. Fuya, Z. Huifen, *Chin. J. Geochem.* 74 (1995) 78.
- [9] S. Lee, Y.J. Kim, H.S. Moon, *J. Am. Ceram. Soc.* 82 (1999) 2841.
- [10] D. Massiot, P. Dion, J.F. Alcover, F. Bergay, *J. Am. Ceram. Soc.* 78 (1995) 2940.
- [11] W.M. Brown, K.J.D. Mackenzie, M.E. Bowden, R.H. Meinhold, *J. Am. Ceram. Soc.* 68 (1985) 298.
- [12] L.H. Merwin, A. Sebal, H. Rager, H. Schneider, *Phys. Chem. Miner.* 18 (1991) 47.
- [13] C.I. Fialips, A. Navrotsky, S. Petit, *Am. Mineral.* 86 (2001) 304.
- [14] B.L. Sherriff, H.D. Grundy, *Nature* 332 (1988) 819.
- [15] W.E. Cameron, *Am. Mineral.* 62 (1977) 747.
- [16] J. Angel, C.T. Prewitt, *Am. Mineral.* 71 (1986) 1476.
- [17] U.C. Bertram, V. Heine, I.L. Jones, G.D. Price, *Phys. Chem. Miner.* 17 (1990) 326.
- [18] R. Blinc, *Phys. Rep.* 79 (1981) 331.